Biology

Biology fields

Okayama University *Year* 2006

Identification of glycosylation genes and glycosylated amino acids of flagellin in Pseudomonas syringae pv. tabaci

Fumiko Taguchi, *Okayama University*
Kasumi Takeuchi, *Okayama University*
Etsuko Katoh, *National Institute of Agrobiological Sciences*
Katsuyoshi Murata, *National Institute of Agrobiological Sciences*
Tomoko Suzuki, *Okayama University*
Mizuri Marutani, *Okayama University*
Takayuki Kawasaki, *Okayama University*
Minako Eguchi, *Okayama University*
Shizue Katoh, *National Institute of Agrobiological Sciences*
Hanae kaku, *National Institute of Agrobiological Sciences*
Chihiro Yasuda, *Okayama University*
Yoshishige Inagaki, *Okayama University*
Kazuhiro Toyoda, *Okayama University*
Tomonori Shiraishi, *Okayama University*
Yuki Ichinose, *Okayama University*

i) Title: **Identification of glycosylation genes and glycosylated amino acids of flagellin in *Pseudomonas syringae* pv. *tabaci***

ii) Author's names: Fumiko Taguchi,[1§] Kasumi Takeuchi,[1,2§] Etsuko Katoh,[2] Katsuyoshi Murata,[2] Tomoko Suzuki,[1] Mizuri Marutani,[1] Takayuki Kawasaki,[1] Minako Eguchi,[1] Shizue Katoh,[2] Hanae Kaku,[2†] Chihiro, Yasuda,[1] Yoshishige Inagaki,[1] Kazuhiro Toyoda,[1] Tomonori Shiraishi[1] and Yuki Ichinose[1*]

iii) Affiliations and addresses: [1]The Graduate School of Natural Science and Technology, Okayama University, Tsushima-naka 1-1-1, Okayama 700-8530 Japan. [2]National Institute of Agrobiological Sciences, Kannondai 2-1-2, Tsukuba, Ibaraki 305-8602, Japan.

iv) *For correspondence: E-mail yuki@cc.okayama-u.ac.jp; Tel. and FAX (+81) 86 251 8308.

v) Running title: Glycosylation of *P. syringae* pv. *tabaci* flagellin

vi) Key words: Elicitor, Flagellin, Glycosylation island, Hypersensitive reaction, Protein glycosylation

vii) Footnotes: The nucleotide sequence reported in this paper has been submitted to the DDBJ/GenBank/EMBL databank and has been assigned accession number AB061230.

[§] The first two authors contributed equally to this work.

[†] Present address: Faculty of Agriculture, Meiji University, Kawasaki, Kanagawa 214-8571

Japan.

Summary

A glycosylation island is a genetic region required for glycosylation. The glycosylation island of flagellin in *P. syringae* pv. *tabaci* 6605 consists of three *orfs*: *orf1*, *orf2* and *orf3*. *Orf1* and *orf2* encode putative glycosyltransferases, and their deletion mutants, Δ*orf1* and Δ*orf2*, exhibit deficient flagellin glycosylation or produce partially glycosylated flagellin, respectively. Digestion of glycosylated flagellin from wild-type bacteria and non-glycosylated flagellin from Δ*orf1* mutant using aspartic *N*-peptidase and subsequent HPLC analysis revealed candidate glycosylated amino acids. By generation of site-directed Ser/Ala-substituted mutants, all glycosylated amino acid residues were identified at positions 143, 164, 176, 183, 193 and 201. MALDI-TOF MS analysis revealed that each glycan was about 540 Da. While all glycosylation-defective mutants retained swimming ability, swarming ability was reduced in the Δ*orf1*, Δ*orf2* and Ser/Ala-substituted mutants. All glycosylation mutants were also found to be impaired in the ability to adhere to a polystyrene surface and in the ability to cause disease in tobacco. Based on the predicted tertiary structure of flagellin, S176 and S183 are expected to be located on most external surface of the flagellum. Thus the effect of Ala-substitution of these

serines is stronger than that of other serines. These results suggest that glycosylation of flagellin in *P. syringae* pv. *tabaci* 6605 is required for bacterial virulence. It is also possible that glycosylation of flagellin may mask elicitor function of flagellin molecule.

Introduction

While prokaryotes have long been thought incapable of glycosylating proteins, it has recently become apparent that protein glycosylation is not restricted to eukaryotes (Benz and Schmidt, 2002; Power and Jennings, 2003; Schmidt *et al.*, 2003). It is known that several surface-layer proteins, pilin and flagellin, are glycosylated in many pathogenic bacteria. Because these proteins are surface-exposed, it is likely that they associate directly with host factors. Flagellin glycosylation has been found in many animal pathogens such as *Campylobacter jejuni* and *Pseudomonas aeruginosa*, and some of the glycan structures have been identified (Arora *et al.,* 2001; Schirm *et al.,* 2004; Thibault *et al.,* 2001). In the case of *P. aeruginosa* strain PAK, a glycan consisting of 11 monosaccharides is linked to flagellin protein by rhamnose, and two identified glycosylation sites were localized to the central domain (Schirm *et al.,* 2004). Thibault *et al.* (2001) reported that the glycan structure of flagellin in *C. jejuni* has uncommon carbohydrate residues, pseudaminic acid and its derivatives. Flagellin glycosylation is also found

in plant pathogens such as *P. syringae* pv. *tabaci* 6605, pv. *glycinea* and pv. *tomato* (Taguchi *et al.,* 2003a; Takeuchi *et al.,* 2003) and *Acidovorax avenae* (Che *et al.,* 2000).

Flagellin is known as an immunodominant protein recognized during infection and has been suggested to be an immunoprotective antigen in *C. jejuni* (Thibault *et al.,* 2001; Guerry *et al.,* 1996). Furthermore, flagellin is capable of inducing an animal defense response via the toll-like receptor 5 (TLR5, Hayashi *et al.,* 2001). Flagellin in plant pathogenic bacteria is also known as a potential elicitor, which is a molecule capable of induction of a plant defense response (Che *et al.,* 2000; Felix *et al.,* 1999; Taguchi *et al.,* 2003b). Interestingly, we found that flagellin proteins from *P. syringae* pv. *glycinea* race 4 and pv. *tomato* DC3000 are able to induce a rapid and strong plant defense response, the so-called hypersensitive reaction (HR), which is accompanied by programmed cell death of non-host tobacco cells. However, flagellin from a tobacco pathogen, *P. syringae* pv. *tabaci* 6605*,* did not induce HR in tobacco (Taguchi *et al.,* 2003b). Nevertheless, the deduced amino acid sequences of flagellin from *P. syringae* pv. *tabaci* 6605 and pv. *glycinea* race 4 are identical. Further, the purified flagellin in the Δ*fliC* mutant of *P. syringae* pv. *tabaci* 6605*,* which possesses a heterologous *fliC* gene derived from *P*. *syringae* pv. *glycinea* race 4 and pv. *tomato* DC3000, did not induce HR cell death in tobacco cells (Taguchi *et al.,* 2003a). These results suggest that the HR-inducing ability of flagellins is determined by

post-translational modification. Recently, we found that putative genes for glycosyltransferase are required for flagellin glycosylation in *P. syringae* pv. *glycinea* race 4, and deletion of some resulted in the production of non-glycosylated or incompletely-glycosylated flagellins (Takeuchi *et al.,* 2003). Further, the deletion of putative glycosyltransferase genes for flagellin reduced virulence toward host soybean plants and HR-inducing ability in non-host tobacco plants (Takeuchi *et al.,* 2003). These results indicate that flagellin glycosylation plays an important role in determining host and non-host interactions between plants and *P. syringae*. Thus, it is plausible that glycosylation of surface-exposed proteins like flagellin is an acquired mechanism that has evolved in order to avoid plant recognition.

It is known that bacterial *hrp* (hypersensitive response and pathogenicity) genes are required for the induction of plant HR. However the Δ*fliC* mutant of *P. syringae* pv. *tabaci* 6605 almost lost HR-inducing ability on non-host tomato cells (Shimizu *et al*., 2003) and the Δ*hrcC*, an *hrp*-defective mutant of this pathogen still retained HR-inducing ability on tomato (Marutani *et al.,* 2005). These results indicate that flagellin of this pathogen induced HR on its non-host plants in *hrp*-independent manner and thus flagellin is a major HR elicitor in this pathogen.

In this study, we analyzed genes required for flagellin glycosylation, the so-called "glycosylation island," in *P. syringae* pv. *tabaci* 6605. Further, we identified the glycosylated

amino acid residues and molecular size of the glycan in flagellin. We also generated flagellin glycosylation mutants through amino acid substitutions. Using these mutants, we investigated bacterial behavior, virulence and HR-induction activity to clarify the role of glycosylation in bacterial virulence and in interactions with plants.

Results

Sequence analysis and genetic organization of the glycosylation island in P. syringae *pv.* tabaci *6605*

We determined the genomic sequence of the putative glycosylation island located upstream of the *fliC* gene of *P. syringae* pv. *tabaci* 6605 using an isolated phage clone (Fig 1A). The sequence data revealed three *orf*s, designated *orf1, orf2* and *orf3*, between *flgL*, which encodes flagellar hook-associated protein 3, and *fliC* as we originally found in *P. syringae* pv. *glycinea* race 4 (Takeuchi *et al.,* 2003). The proteins encoded by *orf1* and *orf2* had predicted molecular masses of 134 and 111 kDa, respectively, and both proteins showed homology to OrfN protein in the region of the glycosylation island of *P. aeruginosa* (Arora *et al.,* 2001) and to RfbC, a protein involved in biosynthesis of O-antigen in *Myxococcus xanthus* (Guo *et al.,* 1996), suggesting that they may be glycosyltransferases. The amino acids sequences encoded by

orf1 and *orf2* share 28% homology. On the other hand, *orf3* potentially encodes a 33 kDa protein that shows significant homology to the putative 3-oxoacyl-(acyl carrier protein) synthase III of *P. putida* strain KT2440 (Nelson *et al.,* 2002) and to the *orfC* product of *P. aeruginosa* strain PAO1 (Arora *et al.,* 2001).

Characterization of the* Δorf1, Δorf2 *and* Δorf3 *mutants of* P. syringae *pv.* tabaci *6605

To analyze the role of these putative glycosyltransferases, deletion mutants of each *orf* were constructed in *P. syringae* pv. *tabaci* 6605 as described in the experimental procedures and northern analysis was performed using *orf*-specific probes to confirm non-polarity of the mutations. The results demonstrated that the Δ*orf1*, Δ*orf2* and Δ*orf3* mutants are non-polar (Fig. 1B). After purification of flagellins from wild-type (WT) and from the Δ*orf1*, Δ*orf2* and Δ*orf3* mutants, SDS-PAGE was carried out (Fig. 1C). The molecular mass decreased in the Δ*orf1* and the Δ*orf2* mutants, suggesting that these genes are necessary for the glycosylation of flagellin protein. However, the Δ*orf3* mutant produced flagellin with a size identical to that of wild-type.

A glycoprotein-staining experiment was performed to compare the glycosylation status of flagellins from each strain (Fig. 1D). The glycosylation of flagellin prepared from the Δ*orf*3 mutant was clearly detected at almost the same level as from wild-type. Although the flagellin from the Δ*orf2* mutant was glycosylated, the glycostaining was found to be weaker than flagellin

from wild-type and Δ*orf3* mutant. In contrast, flagellin from the Δ*orf1* mutant did not stain as a glycoprotein, indicating no glycosylation.

To confirm the necessity of *orf1* and *orf2* for the increase of flagellin in size, the complete glycosylation island was introduced into the Δ*orf1,* Δ*orf2* and Δ*orf3* mutants. As shown in Fig. 1E, the reduction in molecular mass in these mutants was complemented when this region was provided, whereas the introduction of the vector control had no effect. Although the Δ*orf3* mutant was also complemented by this region, the Δ*orf3* mutant produced flagellin with a size identical to that of wild-type, thus no effect on mobility was observed.

Identification of modified residues in flagellin of* P. syringae *pv.* tabaci *6605

To determine the location of glycosylated residues, purified flagellin proteins from wild-type and from the Δ*orf1* mutant of *P. syringae* pv. *tabaci* 6605 were digested with aspartic *N*-peptidase and analyzed by HPLC. As shown in Fig. 2, when the retention times of peptide fragments produced by this treatment were compared, three specific peaks (fractions 41, 50 and 66) were detected only in the chromatogram of wild-type flagellin. *N*-terminal sequencing analysis revealed that these fragments were 41-1: residues 200 through 211 (DSALQTINSTRA), 41-2: residues 70 through 78 (DGMSLAQTA), 50-1: residues 23 through 42 (DALSTSMTRLSSGLKINSAK), 50-2: residues 168 through 187

(DANTLGVGSAVTIAGSDSTT), 66-1: residues 189 through 199 (ETNFSAAIAAI), and 66-2: residues 139 through 167 (DGSASTMTFQVGSNSGASNQITLTLSASF). In this sequencing analysis, residues S143 (66-2), S176, S183 (50-2), S193 (66-1) and S201 (41-1) were not identified by incorrect retention times, suggesting that these amino acids are likely to be modified. Because amino acids S164-F167 were relatively distant from the sequencing start point at D139, it was not possible to determine whether S164 and S166 were modified by the peptide sequencing experiment. Consequently, in addition to five serines at 143, 176, 183, 193 and 201, serines at 164 and 166 are candidates for glycosylation.

Site-directed mutagenesis of putative glycosylated residues of* P. syringae *pv.* tabaci *6605

To confirm whether these residues are necessary for glycosylation, candidate serines were replaced with alanine residues using a QuikChange XL site-directed mutagenesis kit. As shown in Fig. 3, monomeric flagellin proteins from each single Ser/Ala-substituted mutant (S143A, S164A, S176A, S183A, S193A and S201A, respectively) indicate a lower molecular mass than that of the wild-type strain. Although the S166A mutant was also examined by SDS-PAGE, the molecular mass of this flagellin was not reduced, indicating that this position was not modified (data not shown). The six serine-substituted mutant (S143A, S164A, S176A, S183A, S193A and S201A) had a mass of approximately 29 kDa, the same as that of the Δ*orf1*

mutant by SDS-PAGE analysis. These results are consistent with the possibility that the six serine residues present at 143, 164, 176, 183, 193 and 201 are glycoslyated in flagellin from *P. syringae* pv. *tabaci* 6605.

MS spectrometry of flagellin proteins from* P. syringae *pv.* tabaci *6605

To obtain more precise information about the flagellin proteins, the monomeric flagellin and lysyl endopeptidase-digested flagellin peptides were subjected to matrix-assisted laser desorption/ionization time of flight (MALDI-TOF) mass spectrometry (MS) (Fig. 4, Table 1). Mass spectral analyses of intact flagellin purified from the wild-type strain revealed major $[M+H]^+$ signals at 32382 Da and 32529 Da, reflecting heterogeneity in glycoform distribution of the *P. syringae* pv. *tabaci* 6605 flagellin. These molecular masses were 3234 Da or 3381 Da larger than that predicted from the *fliC* sequence, $[M+H]^+$ = 29148 Da.

In a lysyl endopeptidase-digested peptide mixture from the wild-type strain, ions observed at 15301 Da and 15447 Da corresponded to the peptide Asn^{136}-Lys^{255}, for which the predicted value is 12074 Da, supplemented with molecular masses of 3227 Da and 3373 Da, respectively. Thus, the molecular mass of glycans observed in intact flagellin and in the Asn^{136}-Lys^{255} peptide are nearly identical, indicating that all modified residues are located within this peptide. The molecular masses of both intact flagellin and the peptide Asn^{136}-Lys^{255} of the

Δ*orf1* mutant are almost identical to the molecular masses predicted from the deduced amino acid sequences, indicating that the flagellin of the Δ*orf1* mutant is not glycosylated. In the case of the flagellin purified from the Δ*orf2* mutant, the ion spectrum of peptide Asn^{136}-Lys^{255} showed a broad signal distribution, extending from 12220 Da to 14367 Da with more than 15 peaks. Two major molecular masses of peptide Asn^{136}-Lys^{255} observed in the wild-type strain and in the Δ*orf3* mutant were also nearly identical, around 15300 Da and 15446 Da, indicating that the flagellin of the Δ*orf3* mutant is identical to that of the wild-type strain.

MS analysis of flagellins purified from all of the Ser/Ala-substituted mutants was also carried out. Flagellins of single Ser/Ala-substituted mutants exhibited heterogeneous patterns that included an additional peak that was larger than the main peak by approximately 145 Da, like those of wild-type and the Δ*orf3* mutant. MS data for flagellin from the S143A mutant are shown in Fig. 4 as a representative of single Ser/Ala substituted mutants. Substitution of each serine by alanine decreased the molecular mass of flagellin by about 540 Da (Table 1).

To evaluate the linkage of glycosylation of Asn^{136}-Lys^{255} peptide of flagellin from *P. syringae* pv. *tabaci* 6605, ß-elimination was carried out by using NH_4OH. The predicted molecular mass of Asn^{136}-Lys^{255} peptide should be 12068 Da, which is a calculated value from the deduced amino acid sequence. After treatment of a lysyl endopeptidase-digested peptide with

NH_4OH, a major peak was observed at 12071.2 Da instead of 15301 Da and 15447 Da that were observed in untreated peptide (Fig. 4). This result suggests that all glycosylation sites in Asn^{136}-Lys^{255} peptide are *O*-linked. Furthermore, a minor peak was also observed at 12610.6, indicating less amount of glycan remained. The difference of molecular masses between 12071.2 and 12610.6 is 539.4, which is consistent with the molecular mass of glycan in one serine as calculated in Table 1.

Homology model of flagellin from* P. syringae *pv.* tabaci *6605

Site-directed mutagenesis and MS analysis of flagellin from *P. syringae* pv. *tabaci* 6605 showed that the six serine residues: S143, S164, S176, S183, S193 and S201 were glycosylated. In order to visualize these sites, the three-dimensional structure of flagellin from *P. syringae* pv. *tabaci* 6605 was modeled. The three-dimensional structure of bacterial flagellar filament has been determined by X-ray diffraction (Samatey *et al.*, 2001) and electron cryomicroscopy (Yonekura *et al.*, 2003) in *Salmonella typhimurium*. Samatey *et al*. reported the crystal structure of a 41kDa flagellin fragment (F41) composed of three domains, D1, D2 and D3. Recently, Yonekura *et al*. reported the whole structure of flagellin (D0-D3). Sequence alignment of flagellin from *P. syringae* pv. *tabaci* 6605 and from *S. typhimurium* is shown in Fig. 5A. These proteins show high similarity, especially within the D0 and D1 domains. Flagellin

from *P. syringae* pv. *tabaci* 6605 shares 56.0% identity and 63.0% similarity in the D0 domain, and 45.8% identity and 53.5% similarity in the D1 domain from *S. typhimurium* flagellin. The D2 and D3 domains are missing in flagellin from *P. syringae* pv. *tabaci* 6605*,* except for a small portion of D3 (L163-S183).

The tertiary structure of flagellin from *P. syringae* pv. *tabaci* 6605 was predicted by Modeller just as the F41 fragment structure of the *Salmonella* flagellin (1IOI) was predicted (Fig. 5B). The predicted structure of flagellin, especially that of D1 is similar to that of *S. typhimurium*. It has three long α-helixes (α1:I58-R100, α2:S106-S129, α3:A195-A234) and one short β-sheet composed of two β-strands (β1:S143-Q148, β2:S156-L161). There is no D2 domain. As shown in Fig. 5B, the glycosylation sites are mapped in the predicted structure. Of the six glycosylation sites, the four serine residues (S164, S176, S183 and S193) are located in the loop between β2 and α3, and S193 is located at the edge of β1 as shown in Fig. 5B. Although S201 is located at α3 in D1, its position is on the outside surface of the molecule as are all the other glycosylation sites. This structure suggests that sugar chains may be functionally important and may behave like the D2 and D3 domains.

Swimming, swarming motility and adhesion of glycosylation mutants

Swimming and swarming motility of wild-type and glycosylation-defective mutants

were examined on 0.3 % soft agar MMMF plates and on 0.5 % semi-solid agar SWM plates, respectively (Fig. 6A). The Δ*fliC* mutant completely lost not only swimming motility (Shimizu *et al.,* 2003) but also swarming motility. Although swimming motility was not affected by deletion of the glycosylation island and the Ser/Ala-substitutions (data not shown), swarming motility was greatly affected by the mutations. The Δ*orf3* mutant retained the wild-type or higher level of swarming motility, whereas the Δ*orf1*, Δ*orf2* and all Ser/Ala-substituted mutants had reduced swarming ability. An especially significant reduction in swarming motility was observed in the Δ*orf1* and Δ*orf2* mutants, in S176A, S183A, and in the six serine-substituted mutant.

We also examined adhesion. All of the mutants examined had a reduced ability to attach to a polystyrene surface relative to that of wild-type, especially the Δ*orf1* mutant, S176A, S183A and S193A, each single Ser/Ala-substituted mutant, and the six serine-substituted mutant (Fig. 6B). There was statistically significant difference in adherent ability between wild-type and each mutant (the largest *P* value, 0.0029 for Δ*orf3*; *P* values for other mutants are <0.0001).

Detection of mucoid substances on inoculated tobacco leaves by scanning electron microscopy

To examine whether the formation of extracellular polymeric substance (EPS) matrix in wild-type is different from that in the Δ*orf1* mutant, the surface of tobacco leaves inoculated

with *P. syringae* pv. *tabaci* 6605 was observed by scanning electron microscopy. As shown in Fig. 7, the wild-type bacteria were embedded in the matrix in crevices on the leaf surface after 8 days inoculation, and mucoid matrix with peelings were found in the vicinity similar to the biofilm-like structure reported previously (Björklöf *et al.,* 2000). On the other hand, mucoid materials were rarely detected in the area surrounding the Δ*orf1* mutant.

Virulence and growth of mutants on host tobacco leaves

We performed an inoculation test with the glycosylation island-deleted mutants and Ser/Ala-substituted mutants to investigate the effects of these mutations on virulence towards host tobacco leaves. Necrotic lesions were observed after 12 days incubation following spray inoculation of the wild-type strain at 2 x 10^8 cfu ml^{-1}. In contrast, all mutants displayed reduced virulence, especially all the Δ*orf* mutants, the S176A and S183A mutants and the six serine-substituted mutant (Fig. 8A). When we inoculated tobacco leaves with these pathogens by an infiltration method at a density of 2 x 10^5 cfu ml^{-1}, all glycosylation-defective mutants resulted in less virulence compared to wild-type. However, differences of the virulence between wild-type and mutants in the inoculation by an infiltration method were not so obvious as those in the inoculation by spraying (data not shown).

Growth of the wild-type, Δ*orf1,* Δ*orf2,* Δ*orf3,* S183A and six serine-substituted

mutants in the spray-inoculated and infiltrated tobacco leaves was also examined. All mutants had less growth than the wild-type strain by 8 days after spray-inoculation as shown in Fig. 8B. However, the difference of bacterial population is not so obvious in the infiltrated tobacco leaves (Fig. 8C). The level of virulence on tobacco leaves shown in Fig. 8A and 8B was found to correlate well with the observed defects in swarming behavior, adhesion ability and growth.

Cell death assay of soybean suspension culture using mutant flagellin protein

To investigate the interactions between a series of mutant strains of *P. syringae* pv. *tabaci* 6605 and a non-host soybean plant, induction of cell death by treatment with purified flagellins was examined (Fig. 9). Flagellin prepared from wild-type *P. syringae* pv. *tabaci* 6605 induced death in approximately 40 % of the cells. In contrast, flagellins prepared from the Δ*orf1* mutant and the six serine-substituted mutant induced death in only about 22% of the cells, and that from *P. syringae* pv. *glycinea* race 4 wild-type induced only about 17% cell death. The percentage of dead soybean cells was also reduced by treatment with flagellin derived from the Δ*orf2* mutant and the single Ser/Ala-substituted mutants. We also examined the cell death-inducing activity of the preparation from the Δ*fliC* mutant to rule out a possibility of the contamination of other elicitor molecules in flagellin fraction. As shown in Fig. 9, there is no significant activity to induce cell death in this preparation. These results indicate that

glycosylation of flagellin is needed by the soybean cultured cells for induction of a wild-type defense response.

Discussion

In this paper, we report genetic and structural analyses of the glycoprotein, flagellin, and of the genes in the glycosylation island of the flagella gene cluster of *P. syringae* pv. *tabaci* 6605, involved in flagellin-glycosylation. Sequence analysis revealed that *orf1* and *orf2* exhibit homology to the putative protein RfbC from *Myxococcus xanthus*, which is involved in O-antigen biosynthesis (Guo *et al.,* 1996). Although the mechanisms of glycosylation of lipopolysaccharide are different from that of flagellin, it is possible that the specificity of bacteria-host interactions may be determined by flagellin glycosylation, similar to the O-antigen reaction. *Orf1, orf2* and *orf3* of *P. syringae* pv. *tabaci* 6605 also exhibited the highest degree of homology to the corresponding genes in *P. syringae* pv. *glycinea* (Takeuchi *et al.,* 2003). At the amino acid level, these *orf*s showed 99.6, 99.3 and 99.7% homology, meaning that only 3, 7, or 1 amino acid residue differed from one another, respectively. Because our previous results demonstrated that post-translational modification of flagellin correlates with the ability to induce HR cell death (Taguchi *et al.,* 2003a, 2003b), these slight differences at the amino acid level may

determine substrate specificity or sugar binding preferences, both of which play crucial roles in the specificity of pathogen-plant interactions. An experiment to replace the glycosylation island in *P. syringae* pv. *tabaci* 6605 with that in *P. syringae* pv. *glycinea* race 4 is in progress to elucidate this possibility.

Immunoblotting and MS analysis of flagellin proteins from the Δ*orf1*, the Δ*orf2* and Ser/Ala-substituted mutants confirmed a reduction in molecular mass. The molecular mass of flagellin from the Δ*orf1* and six-serine-substituted mutants are approximately consistent with that predicted from the *fliC* sequence, suggesting that flagellins from these mutants are not glycosylated (Table 1). On the other hand, the molecular mass of the glycosylated flagellin was heterogeneous. In particular, the molecular mass of flagellin from the Δ*orf2* mutant was quite variable, with a value intermediate between that of wild-type and the Δ*orf1* mutant. The heterogeneity of the Δ*orf2* mutant suggests the possibility that temporal or spatial cooperation between Orf1 and Orf2 is essential for normal maturation of flagellin.

Structural analysis of the flagella filament from *S. typhimurium* revealed that the flagellin monomer is composed of four domains, D0, D1, D2 and D3, and that flagellins are assembled through intermolecular interactions (Yonekura *et al.,* 2003). The highly conserved domains, D0 and most of D1, are not expected to be surface-exposed. The molecular size of

flagellin of the *P. syringae* pathovars is smaller than that of *S. typhimurium* because *P. syringae* flagellin does not possess the corresponding amino acid sequence for the D2 and most of the D3 domains of *S. typhimurium*. All glycosylated amino acids are located in the internally variable D3 domain and in the distal region of D1, which are expected to be on the surface-exposed portion of the flagella filament of *P. syringae* pv. *tabaci* 6605 as shown in Fig. 5 and elsewhere (Ichinose *et al.,* 2004). Thus, the glycans in flagellin seem to be able to associate easily with the plant cell surface. In *P. syringae* pv. *tabaci* 6605*,* all glycans are linked though serine residues at positions 143, 164, 176, 183, 193 and 201. All previously identified glycosylated amino acids in flagellin and pilin of eubacteria were found to be *O*-linked serines or threonines (Thibault *et al*., 2001; Comer *et al.*, 2002; Power and Jennings, 2003; Schirm *et al*., 2004; Schmidt *et al.*, 2003). Thus, *O*-linked glycosylation may be a common feature in flagellin and pilin.

Bacterial swarming discussed in our paper is a flagella-driven movement on 0.5% agar SWM plates, because Δ*fliC* mutant completely lost swarming motility (Fig. 6A). Biofilm formation accompanies EPS matrix with carbohydrates, proteins, peptides and surfactants and observed in members of *Vibrio, Bacillus, Escherichia, Salmonella* and *Pseudomonas* (Daniels *et al*., 2004). Biofilm formation is also involved in virulence. For example, colonization of *P. aeruginosa* is established upon conversion to the mucoid phenotype (Firoved and Deretic, 2003).

Thus mucoid *P. aeruginosa* produces a thick mucopolysaccharide layer consisting of a biofilm, and induces heightened inflammation, tissue destruction and declining pulmonary function in human patients. In the case of phytopathogenic bacteria, biofilm formation and its significance in virulence is not clear at present. In this study, we observed that wild-type bacteria, but not the less virulent strain Δ*orf1*, formed a biofilm-like structure on the surface of a tobacco leaf as assessed by scanning electron microscopy (Fig. 7), similar to the report by Björklöf *et al.* (2000). The ability to adhere and swarming motility of the Δ*orf1*, Δ*orf2* and Ser/Ala-substituted mutants were lower than in wild-type (Fig. 6), and their virulence on host tobacco leaves was also reduced (Fig. 8A). Interestingly, swarming, adhesion and HR induction were all significantly reduced in the single serine-substituted mutants, S176A and S183A, but were less compromised in the S143A, S164A and S201A mutants (Figs. 6 and 9). Based on the predicted tertiary structure of flagellin, S176 and S183 are expected to be located on the external surface of the flagellum. These results suggest that removal of the glycosyl moiety, especially the most surface-exposed glycans, reduced flagella-driven motility, adhesion, and virulence. The effect of the removal of glycosyl moiety on bacterial virulence is prominent in the spray-inoculated tobacco leaves (Fig. 8B) but not obvious in the infiltrated leaves (Fig. 8C). This result indicates that the reduction of virulence of glycosylation-defective mutants dues to their reduced abilities

to swarm and adhere. However, glycosylation is also potential to avoid plant recognition by masking the elicitor domain in flagellin, since the population of wild-type strain was a little higher than others at 8 days after inoculation.

Deletion mutants lacking the putative glycosyltransferases and the Ser/Ala-substituted mutants of *P. syringae* pv. *tabaci* 6605 all had a reduced ability to induce HR cell death in non-host suspension cultured soybean cells (Fig. 9). We have reported elsewhere that the corresponding deletion mutants, Δ*orf1* and Δ*orf2,* of *P. syringae* pv. *glycinea* race 4 had a reduced ability to induce an oxidative burst in non-host tobacco leaves (Takeuchi *et al.,* 2003). Taken together, these results support the idea that flagellin glycosylation is one of the important process in bacterial HR-inducing activity. The three-dimensional structure of the glycosylated motif in flagellin may affect binding affinity by its putative receptor. Another possibility is that glycosylation status may affect bacterial virulence itself. It is reported that protein glycosylation in *C. jejuni* affects interactions with host cells (Szymanski *et al*., 2002). Recently motility and glycosylation of the flagellum were reported to be important determinants of flagellar-mediated virulence in *P. aeruginosa* (Arora *et al.*, 2005). Thus, glycosylation of surface-exposed proteins such as flagellin might serve specific functions in infection and pathogenesis, and interfere with defense responses. Indeed, virulence-related bacterial characteristics such as adhesion and

swarming motility were significantly reduced in most of the glycosylation mutants (Fig. 6).

Flagella are known as essential virulence factors that mediate motility. We observed that flagella-defective mutants of *P. syringae* pv. *tabaci* 6605 had a reduced ability to cause wild-fire disease in host tobacco plants (Ichinose *et al.,* 2003). Flagellin, the major component of the flagella filament functions as one of the pathogen-associated molecular patterns (PAMPs, Hayashi *et al.,* 2001; Gomez-Gomez and Boller 2002), which are recognized at an early stage during infection by the innate immune system.

It is also well known that the synthetic oligopeptide flg22, which was designed from an *N*-terminal conserved sequence in the D0 interior domain of flagellin from *P. aeruginosa*, induced a plant defense response as one of the PAMPs (Felix *et al.* 1999). Further, *FLS2*, a gene encoding the receptor for flg22, was identified in *Arabidopsis thaliana* (Gomez-Gomez and Boller 2000). However, flg22 has been reported to not induce HR cell death, whereas purified flagellin from *P. syringae* is able to induce HR cell death in non-host plants. Thus, the different effects of flg22 and purified flagellin suggest that each elicitor molecule is recognized independently. In other words, the original flagellin may be recognized not only by FLS2 but also by an as-yet unidentified novel receptor. Recently, we reported that *A. thaliana* might have another type of receptor that recognizes flagellin-associated glycan (Ishiga *et al.* 2005).

In bacteria, quorum sensing is a system for bacterium-bacterium communication via small signal molecules, the so-called quorum-sensing molecules or autoinducers. For example, *N*-(3-oxohexanoyl)-L-homoserine lactone, the autoinducer for *Vibrio fischeri,* is produced from S-adenosylmethionine and a 3-oxo-hexanoyl-acyl carrier protein by LuxI synthase (More *et al.,* 1996). *P. syringae* pv. *tabaci* 6605 also produces *N*-(3-oxohexanoyl)-L-homoserine lactone (Shaw *et al.,* 1997). In this connection, it is interesting that *orf3* potentially encodes a 3-oxoacyl-(acyl carrier protein) synthase III homolog that might be involved in fatty acid elongation and formation of a possible precursor of acyl-homoserine lactone, a quorum-sensing molecule (Hoang *et al.,* 2002). *N*-acyl-homoserine lactone has been reported to have no effect on swarming motility in *P. syringae* pv. *syringae* (Kinscherf and Willis, 1999). While the Δ*orf3* mutant retains swimming and swarming motility, its ability to cause disease on host tobacco leaves was reduced significantly. MS analysis indicated that *orf3* is not involved in post-translational modification of flagellin (Table 1). The results described above suggest that other important virulence factors beside motility and flagellar glycosylation must be missing in the Δ*orf3* mutant, although the function of Orf3 is not clear at present.

The structure of the glycosyl moiety of flagellin and the function of putative glycosyltransferases in both *P. syringae* pv. *tabaci* 6605 and pv. *glycinea* race 4 remain to be

elucidated. The flagellin proteins from the mutants of both pathovars will be valuable tools to further investigate and to clarify the role of flagellin-glycosylation in the interactions of flagella with plants.

Experimental procedures

Plant materials

Tobacco plants (*Nicotiana tabacum* L. cv. Xanthi NC) were grown at 25°C with a 12 h photoperiod. The suspension cultured soybean cells (*Glycine max* cv. Enrei) were inoculated every week and were used in the cell death assay when 4 days old (Yokoyama *et al*., 2000).

Bacterial strains and culture conditions

Bacterial strains used in this study are listed in Table 2. *Pseudomonas syringae* pv. *tabaci* 6605 strains were maintained in King's B (KB) medium at 27°C, and *Escherichia coli* strains were grown at 37°C in Luria-Bertani (LB) medium.

Inoculation procedure and bacterial growth

For the spray-inoculation experiment, each bacterial strain was suspended in 10 mM $MgSO_4$ containing 0.02 % Silwet L77 (OSI Specialties Inc., Danbury, Conn) to a density of 2 x 10^8 cfu ml^{-1}. The leaves inoculated on both leaf surfaces were incubated under conditions of

100 % humidity for 1 day and 80 % humidity for 11 subsequent days in a growth cabinet at 23°C. For the inoculation experiment by infiltration method, each bacterial suspension with 10 mM $MgSO_4$ to a density of 2 x 10^5 cfu ml^{-1} was injected into leaves using a needle-less syringe.

To examine the bacterial growth, each inoculated leaf was soaked in 15 % H_20_2 for 1.5 min to sterilize leaf surfaces. Then, five leaf disks (8 mm diameter) were punched from tobacco leaves and ground in a mortar. Serially-diluted samples in 10 mM $MgSO_4$ were spread on KB plates, colonies were counted, and bacterial populations were measured.

Isolation of glycosylation island and generation of mutants

As previously reported, we isolated a phage clone possessing the *fliC* gene from a genomic DNA library of *P. syringae* pv. *tabaci* 6605 (Taguchi *et al*., 2003b; Shimizu *et al*., 2003). An approximately 19-kb phage clone was sequenced (ABI PRISM 310, Applied Biosystems, Chiba, Japan) using a BIG Dye™ terminator cycle sequencing kit.

Mutants of *P. syringae* pv. *tabaci* 6605 that had deletions of each *orf* in the glycosylation island were generated based on homologous recombination according to methods previously described (Takeuchi *et al.,* 2003). PCR primers for the amplification of approximately 1-kb DNA fragments located on each side of the *orfs* were designed based on the relevant sequences in *P. syringae* pv. *glycinea* race 4. In the case of the Δ*orf1* mutant, one of the

primers for the upstream region of Δ*orf1*, called P1UF, was modified as: 5'-GACCAATCGCAGCTATGAAC-3'.

For complementation of the Δ*orf1*, Δ*orf2* and Δ*orf3* mutants, a 9-kb HindIII fragment that contains the complete glycosylation island consisting of *orf1*, *orf2* and *orf3* was inserted into the HindIII site of pDSK519, a broad-host-range plasmid vector (Keen *et al.*, 1988) to construct pDSKGI. pDSKGI was introduced into the Δ*orf1*, Δ*orf2* and Δ*orf3* mutants by conjugation via *E. coli* S17-1.

RNA isolation and northern blot analysis

Wild-type, Δ*orf1*, Δ*orf2* and Δ*orf3* mutants of *P. syringae* pv. *tabaci* 6605 were incubated in KB medium for 24 h at 27°C and total RNA was extracted (High Pure RNA isolation Kit, Roche, Mannheim, Germany) according to the manufacture's protocol. The probes specific for each *orf* were amplified and labeled by a PCR DIG Synthesis Kit (Roche). Ten micrograms of RNA were used for northern blot analysis. Conditions for hybridization and detection have been described (Sasabe *et. al*. 2000).

Site-directed mutagenesis of glycosylated residues of flagellin from* P. syringae *pv.* tabaci *6605

To introduce the desired point mutations, a QuikChange XL site-directed mutagenesis

kit (Stratagene, La Jolla, CA) was used. The *fliC* region was amplified by PCR with PC5 (5'-CGGGATCCAAACCAACGAGGAATTCA-3') and PC6 (5'-CGGGATCCTTACTGAAGCAGTTTCAGTACA-3') primers and was inserted into pBluescript SK^- vector via the BamHI site. This double-stranded DNA vector was used as the template. Two complementary oligonucleotides containing the mutation: 143SA5' (5'-CGACGGTTCCGCCGCCACCATGACTTTCC-3') and 143SA3' (5'-GGAAAGTCATGGTGGCGGCGGAACCGTCG-3'), 164SA5' (5'-GATCACTCTGACTCTGGCCGCAAGCTTCGACGCC-3') and 164SA3' (5'-GGCGTCGAAGCTTGCGGCCAGAGTCAGAGTGATC-3'), 176SA5' (5'CCCTGGGTGTCGGTGCGGCTGTGACCATC-3') and 176SA3' (5'-GATGGTCACAGCCGCACCGACACCCAGGG-3'), 183SA5' (5'-GACCATCGCTGGTGCCGATAGCACCACTGC-3') and 183SA3' (5'-GCAGTGGTGCTATCGGCACCAGCGATGGTC-3'), 193SA5' (5'-GCAGAGACCAACTTCGCTGCCGCTATCGCC-3') and 193SA3' (5'-GGCGATAGCGGCAGCGAAGTTGGTCTCTGC-3'), 201SA5' (5'-CGCCGCCATCGACGCGGCTCTGCAGACC-3') and 201SA5' (5'-GGTCTGCAGAGCCGCGTCGATGGCGGCG-3') were synthesized. Temperature cycling,

DpnI digestion and transformation were performed according to the manufacturer's protocols. The desired mutations were confirmed by DNA sequence analysis, and each *fliC* fragment was inserted into the mobilizable cloning vector pK18*mobsacB* (Schäfer *et al.,* 1994). The resulting plasmids were introduced into *E. coli* S17-1 by electroporation and were integrated into wild-type *P. syringae* pv. *tabaci* 6605 by conjugation. After loss of the plasmid by incubation on KB agar plates containing 12% sucrose, each mutation in the bacteria was confirmed by sequencing and designated 6605-S143A, 6605-S164A, 6605-S176A, 6605-S183A, 6605-S193A and 6605-S201A, respectively. Mutant (6605-6 S/A) with six serine substitutions (6605-S143A, S164A, S176A, S183A, S193A and S201A) was also constructed by the same method.

Purification of flagellin proteins

P. syringae pv. *tabaci* 6605 was inoculated in LB containing 10 mM $MgCl_2$ for 48 h at 25°C. Cells collected by centrifugation were resuspended in 1/3 volume of minimal medium (MM; 50 mM potassium phosphate buffer, 7.6 mM $(NH_4)_2SO_4$, 1.7 mM $MgCl_2$ and 1.7 mM NaCl, pH 5.7) supplemented with 10 mM each of mannitol and fructose (MMMF medium) for 24 h at 23°C. After incubation, the culture was centrifuged at 7,000 x *g* for 10 min, and bacterial flagella were separated from the cells by vortexing for 1 min. After centrifugation at 7,000 x *g* for 10 min, the supernatant was filtered through a 0.45 μm-pore-size filter and centrifuged at

100,000 x *g* for 30 min. The pellet of purified flagellin was suspended in dH_2O at a final concentration of 100 μg ml^{-1}. The same purification procedure was performed in the Δ*fliC* mutant and resultant pellet was diluted by dH_2O with the same ratio for flagellin preparation from wild-type strain. The obtained samples were used for the cell death assay. For MS, purified flagellin was dissociated in 0.1 M glycine-HCl buffer (pH 2.0) and centrifuged at 100,000 x *g* for 30 min. The buffer in the supernatant was replaced with dH_2O by use of a spin column (Centricon YM-30, Amicon, Beverly, MA, USA).

Detection of glycoproteins

After SDS-PAGE of the purified flagellins, glycoproteins were detected by using a GelCode glycoprotein detection kit (Pierce, Rockford, IL) according to the manufacturer's instructions.

Immunoblot analysis

Bacterial cells from *P. syringae* pv. *tabaci* 6605 were prepared as described (Taguchi *et al.* 2003b). Purified flagellin proteins from wild-type and mutant strains of *P. syringae* pv. *tabaci* 6605 were separated by SDS-PAGE and electroblotted onto a PVDF membrane (Amersham Pharmacia Biotech, Buckinghamshire, England). After SDS-PAGE, flagellin protein was detected by an anti-flagellin first antibody and goat anti-mouse second antibody conjugated

with horseradish peroxidase (Taguchi *et al.,* 2003b).

Amino acid sequencing of endopeptidase-digested flagellin

After incubation of flagellin with aspartic *N*-peptidase (Boehringer Mannheim, Mannheim, Germany) at 35°C for 20 h in Tris-HCl buffer (pH 8.0), the resultant peptides in 0.1% (v/v) trifluoroacetic acid (TFA) were subjected to RP-HPLC using a 2.0 x 250 mm TSKgel ODS-80TS column (TOSOH, Tokyo, Japan). Peptides were eluted according to the following program using Solutions A, 0.1% (v/v) TFA, and B, 0.09% (v/v) TFA in 90% (v/v) acetonitrile: (1) 0-2 min, Solution A; (2) 2-7 min, increasing linear gradient from 100% Solution A to 10% (v/v) Solution B; (3) 7-82 min, increasing linear gradient from the second step to 50% (v/v) Solution B; (4) 82-87 min, increasing linear gradient from the third step to 100% (v/v) Solution B; (5) 87-92 min, Solution B; (6) 92-97 min, decreasing linear gradient to Solution A. Elution was monitored at 210 nm. The *N*-terminal amino acid sequence of the detected fragments was analyzed with a protein sequencer (Procise 494 HT protein sequencing system, Applied Biosystems).

Mass spectrometry

All mass spectra were obtained on a Biflex III MALDI-TOF mass spectrometer (Bruker, Ibaraki, Japan) in a linear, positive mode with mass accuracy of 0.2%. Sample solutions

were prepared in water containing 0.1% TFA. All samples were prepared by a dried droplet method, mixing the analyte (intact protein or peptide mixture) with an equal volume of matrix solution [a saturated solution of sinapinic acid in 33% acetonitrile/water with 0.1% TFA (v/v)] and depositing the mixture on a stainless steel target plate. For the preparation of peptide mass measurements, the monomeric flagellin proteins were incubated at 37°C overnight with lysyl endopeptidase (WAKO, Osaka, Japan) [the protein/lysyl endopeptidase, 100:1 (w/w) in 10 mM Tris-HCl buffer (pH 9.0)].

ß-Elimination of glycopeptide

ß-elimination was carried out by using NH_4OH, which is suitable for the following mass spectrometry analysis (Rademaker *et al.*, 1998). The monomeric flagellin protein (100 pmol) were incubated with lysyl endopeptidase in the manner described in "*Mass spectrometry*" at 37°C for overnight. The buffer was replaced with dH_2O using a spin column (Amicon Ultrafree-MC 10,000 NMWL Filter Unit, Millipore, Bedford, MA, USA). The peptide solution was evaporated and dissolved in 500 µl of 28-30% NH_4OH (Sigma Aldrich, St. Louis, MO, USA) and incubated at 45°C for 12 h. The reaction was then stopped by removing the reagent using a vacuum centrifuge. The sample was dissolved in dH_2O and applied to a spin column again for the following examination by MALDI TOF-MS analysis.

Modeling of the three-dimensional structure of flagellin

Flagellin was modeled using version 4.0 of the MODELER program (Ali *et al*., 1993) based on a distance restraint algorithm using spatial restraints extracted from a multiple alignment of the target sequences with the template structure, and from the CHARMM-22 force field. The closest crystalline structure of F41 from *Salmonella* flagellin, Protein Data Bank entry 1IOI (Samatey *et al*., 2001), was used as a template structure. A bundle of five models from random generation of the starting structure was calculated for the sequence. A representative model with the lowest MODELLER target function value was displayed using MOLMOL (Koradi *et al.*, 1996).

Motility assay

For the swimming assay, bacterial cells grown on KB plates were inoculated onto 0.3 % agar MMMF plates with an applicator stick and incubated for 40 h at 23°C. For the swarming assay, bacterial strains were incubated in LB medium containing 10 mM $MgCl_2$ at 27°C for 24 h. After adjusting to an OD_{600} of 1.0 with 10 mM $MgSO_4$, 2 μl aliquots were spotted onto SWM plates (0.5% peptone, 0.3% yeast extract and 0.5% agar; DIFCO, Detroit, MI, USA) at 27°C for 24 h (Kinscherf and Willis, 1999).

Adhesion experiment

Adhesion ability was examined according to the method described by O'Toole and Kolter (1998) with the following modifications. Each bacterial strain was grown in LB medium containing 10 mM $MgCl_2$ at 27°C for 24 h. The density of cell cultures was adjusted to an OD_{600} of 0.1 with fresh MMMF, and 200 µl aliquots were transferred to polystyrene microtiter plate wells (353915, Becton Dickinson, NJ, USA). After incubation at 27°C for 48 h, loosely-bound bacteria were removed by washing with dH_2O three times followed by drying of the plates for 45 min. Adherent bacteria were stained by addition of 200 µl 0.5% crystal violet for 45 min and washed five times with dH_2O. Two hundred µl of 95% ethanol were added to the wells and OD_{595} values were measured.

Detection of cell death

Four-day-old suspension-cultured soybean cells were treated with purified flagellin from each strain at a concentration of 0.32 µM or with dH_2O as control at 23°C on a rotary shaker at 110 rpm. Cell death-inducing activity of the preparation from the Δ*fliC* mutant was also examined. After 18 h incubation, dead cells stained with 0.05 % Evans blue were counted under a light microscope. The percentage of dead cells among a total of one thousand counted cells was calculated. Four independent experiments were performed.

Scanning electron microscopy (SEM)

Samples for scanning electron microscopy were prepared from leaves 8 days post-inoculation. Pre-fixation was done with 3 % (v/v) glutaraldehyde in 0.067 M sodium phosphate buffer (pH 7.4) for 30 min at room temperature. After washing three times in distilled water, samples were post-fixed in 0.5 % (w/v) osmium tetroxide in the same buffer for 0.5 h and were washed again three times in distilled water. The samples were treated with 0.2 % tannic acid for 30 min, washed three times by distilled water and fixed again in 0.5 % (w/v) osmium tetroxide for 15 min and washed again. Specimens were dehydrated through a graded ethanol series, subjected to critical point drying in isoamyl acetate for 30 min, and then mounted on stubs coated with platinum, and examined by scanning electron microscopy (Hitachi S-800, Tokyo, Japan).

Statistical analysis

The results of adhesion assay, cell death assay and bacterial population measurement are expressed as means ± standard deviations. Comparisons of quantitative measurements between wild-type and each mutant were carried out by the two-tailed t-test. P value < 0.01 was considered statistically significant.

Acknowledgments

We thank Dr. A. Collmer (Cornell University, U.S.A.) and Japan Tobacco Inc., Leaf Tobacco Research Laboratory for providing *P. syringae* pv. *glycinea* and pv. *tabaci* 6605, respectively. We are also grateful to Dr. Y. Kimura (Okayama University, Japan) and Dr. S. Aizawa (CREST Soft Nano-machine Project, Japan) for valuable discussions and Dr. T. Yokoyama (Tokyo University of Agriculture and Technology, Japan) for providing the cultured soybean cells. This work was supported in part by Grants-in-Aid for Scientific Research on Priority Area (A) (Nos. 12052215, 12052219) and for Scientific Research (S) (No. 15108001) from the Ministry of Education, Culture, Sports, Science and Technology of Japan and Okayama University COE program "Establishment of Plant Health Science".

References

Ali, A., and Blundell, T. L. (1993) Comparative protein modeling by satisfaction of spatial restraints. *J. Mol. Bi*ol. **234**: 779-815.

Arora, S.K., Bangera, M., Lory, S., and Ramphal, R. (2001) A genomic island in *Pseudomonas aeruginosa* carries the determinants of flagellin glycosylation. *Proc. Natl. Acad. Sci. USA* **98**: 9342-9347.

Arora, S.K., Neely, A.N., Blair, B., Lory, S. and Ramphal, R. (2005) Role of motility and flagellin glycosylation in the pathogenesis of *Pseudomonas aeruginosa* burn would infections. *Infect. Immun.* **73**: 4395-4398.

Benz, I., and Schmidt, M.A. (2002) Never say never again: protein glycosylation in pathogenic bacteria. *Mol. Microbiol.* **45**: 267-276.

Björklöf, K., Nurmiaho-Lassila, E.-L., Klinger, N., Haahtela, K., and Romantschuk, M. (2000) Colonization strategies and conjugal gene transfer of inoculated *Pseudomonas syringae* on the leaf surface. *J. Applied Microbiology* **89**: 423-432.

Che, F.S., Nakajima, Y., Tanaka, N., Iwano, M., Yoshida, T., Takayama, S., *et al.* (2000) Flagellin from an incompatible strain of *Pseudomonas avenae* induces a resistance response in cultured rice cells. *J. Biol. Chem.* **275**: 32347-32356.

Comer, J.E., Marshall, M.A., Blanch, V.J., Deal, C.D., and Castric, P. (2002) Identification of the *Pseudomonas aeruginosa* 1244 pilinglycosylation site. *Infect. Immun.* **70**: 2837-2845.

Daniels, R., Vanderleyden, J., and Michiels, J. (2004) Quorum sensing and swarming migration in bacteria. *FEMS Microbiol. Reviews.* **28:** 261-289

Felix, G., Duran, J.D., Volko, S., and Boller, T. (1999) Plants have a sensitive perception system for the most conserved domain of bacterial flagellin. *Plant J.* **18**: 265-276.

Firoved, A.M., and Deretic, V. (2003) Microarry analysis of global gene expression in mucoid *Pseudomonas aeruginosa*. *J. Bacteriol*. **185**: 1071-1081.

Gomez-Gomez, L., and Boller, T. (2000) FLS2: an LRR receptor-like kinase involved in the perception of the bacterial elicitor flagellin in *Arabidopsis*. *Mol. Cell.* **5:** 1003–1011.

Gomez-Gomez, L., and Boller, T. (2002) Flagellin perception: a paradigm for innate immunity. *Trends Plant Sci.* **7**: 251–256.

Guerry, P., Doig, P., Alm, R.A., Burr, D.H., Kinsella, N., and Trust, T.J. (1996) Identification and characterization of genes required for post-translational modification of *Campylobacter coli* VC167 flagellin. *Mol. Microbiol.* **19**: 369-378.

Guo, D., Bowden, M.G., Pershad, R., and Kaplan, H.B. (1996) The *Myxococcus xanthus rfbABC* operon encodes an ATP-binding cassette transporter homolog required for O-antigen biosynthesis and multicellular development. *J. Bacteriol*. **178**: 1631-1639.

Hayashi, F., Smith, K.D., Ozinsky, A., Hawn, T.R., Yi, E.C., Goodlett, D.R., *et al.* (2001) The innate immune response to bacterial flagellin is mediated by Toll-like receptor 5. *Nature* **410**: 1099-1103.

Hoang, T.T., Sullivan, S.A., Cusick, J.K., and Schweizer, H.P. (2002) β-Ketoacyl acyl carrier protein reductase (FabG) activity of the fatty acid biosynthetic pathway is a determining

factor of 3-oxo-homoserine lactone acyl chain lengths. *Microbiology* **148**: 3849-3856.

Ichinose, Y., Shimizu, R., Ikeda, Y., Taguchi, F., Marutani, M., Mukaihara, T., *et al.* (2003) Need for flagella for complete virulence of *Pseudomonas syringae* pv. *tabaci*: genetic analysis with flagella-defective mutants Δ*fliC* and Δ*fliD* in host tobacco plants. *J. Gen. Plant Pathol.* **69**: 244-249.

Ichinose, Y., Taguchi, F., Takeuchi, K., Marutani, M., Ishiga, Y., Inagaki, Y., *et al.* (2004) Bacterial flagellins as elicitors of the defense response. *In* Genomic and Genetic Analysis of Plant Parasitism and Defense (Tsuyumu *et al.* eds.) APS Press (St. Paul Minnesota, USA). p.83-91.

Ishiga, Y., Takeuchi, K., Taguchi, F., Inagaki, Y., Toyota, K., Shiraishi, T., and Ichinose, Y. (2005) Defense responses of *Arabidopsis thaliana* inoculated with *Pseudomonas syringae* pv. *tabaci* wild type and defective mutants for flagellin (Δ*fliC*) and flagellin-glycosylation (Δ*orf1). J. Gen. Plant Pathol.* **71**: 302-307.

Keen, N.T., Tamaki, S., Kobayashi, D., and Trollinger, D. (1988) Improved broad-host-range plasmids for DNA cloning in gram-negative bacteria. *Gene* **70**: 191-197.

Kinscherf, T.G., and Willis, D.K. (1999) Swarming by *Pseudomonas syringae* B728a requires *gacS* (*lemA*) and *gacA* but not the acyl-homoserine lactone biosynthetic gene *ahlI*. *J.*

Bacteriol. **181**:4133-4136.

Koradi, R., Billeter, M. & Wüthrich, K. (1996) MOLMOL: a program for display and analysis of macromolecular structures. *J. Mol. Graph.* **14**: 51-55.

Marutani, M., Taguchi, F., Shimizu, R., Inagaki, Y., Toyoda, K., Shiraisi, T. & Ichinose, Y. (2005) Flagellin from *Pseudomonas syringae* pv. *tabaci* induced *hrp*-independent HR in tomato. *J. Gen. Plant pathol.* **71**: 289-295.

More, M.I., Finger, L.D., Stryker, J.L., Fuqua, C., Eberhard, A., and Winans, S.C. (1996) Enzymatic synthesis of a quorum-sensing autoinducer through use of defined substrates. *Science* **272**: 1655-1658.

Nelson, K.E., Weinel, C., Paulsen, I.T., Dodson, R.J., Hilbert, H., Martins dos Santos, V.A., *et al.* (2002) Complete genome sequence and comparative analysis of the metabolically versatile *Pseudomonas putida* KT2440. *Environ. Microbiol.* **4**:799-808.

O'Toole, G.A., and Kolter, R. (1998) Initiation of biofilm formation in *Pseudomonas fluorescens* WCS365 proceeds via multiple, convergent signalling pathways: a genetic analysis. *Mol. Microbiol.* **28**: 449-61.

Power, P.M., and Jennings, M.P. (2003) The genetics of glycosylation in Gram-negative bacteria. *FEMS Microbiology Letters* **218**: 211-222.

Rademaker, G.J., Pergantis, S.A., Blok-Tip, L., Langridge, J.I., Kleen A. and Thomas-Oates, J.E. (1998) Mass spectrometric determination of the sites of *O*-glycan attachment with low picomolar sensitivity. *Anal. Biochem.* **257**: 149-160.

Samatey, F.A., Imada, K., Nagashima, S., Vonderviszt, F., Kumasaka, T., Yamamoto, M., Namba, K. (2001) Structure of the bacterial flagella protofilament and implications for a switch for supercoiling. *Nature* **410**:331-337.

Sasabe, M., Takeuchi, K., Kamoun, S., Ichinose, Y., Govers, F., Toyoda, K., *et al.* (2000) Independent pathways leading to apoptotic cell death, oxidative burst and defense gene expression in response to elicitin in tobacco cell suspension culture. *Eur. J. Biochem.* **267**: 5005-5013.

Schäfer, A., Tauch, A., Jäger, W., Kalinowski, J., Thierbach, G., and Pühler, A. (1994) Small mobilizable multi-purpose cloning vectors derived from the *Escherichia coli* plasmids pK18 and pK19: selection of defined deletions in the chromosome of *Corynebacterium glutamicum*. *Gene* **145**: 69-73.

Schirm, M., Arora, S.K., Verma, A., Vinogradov, E., Thibault, P., Ramphal, R., and Logan S.M. (2004) Structural and genetic characterization of glycosylation of type a flagellin in *Pseudomonas aeruginosa*. *J. Bacteriol.* **186**: 2523-2531.

Schmidt, M.A., Riley, L.W., and Benz, I. (2003) Sweet new world: glycoproteins in bacterial pathogens. *Trends Microbiol.* **11**: 554-561.

Shaw, P.D., Ping, G., Daly, S.L., Cha, C., Cronan, J.E. Jr., Rinehart, K.L., and Farrand, S.K. (1997) Detecting and characterizing *N*-acyl-homoserine lactone signal molecule by thin-layer chromatography. *Proc. Natl. Acad. Sci. USA* **94**: 6036-6041.

Shimizu, R., Taguchi, F., Marutani, M., Mukaihara, T., Inagaki, Y., Toyoda, K., *et al.* (2003) The Δ*fliD* mutant of *Pseudomonas syringae* pv. *tabaci,* which secretes flagellin monomers, induces a strong hypersensitive reaction (HR) in non-host tomato cells. *Mol. Genet. Genomics* **269**: 21-30.

Szymanski, C.M., Burr, D.H., and Guerry, P. (2002) Campylobacter protein glycosylation affects host cell interactions. *Infect. Immun.* **70**: 2242-2244.

Taguchi, F., Shimizu, R., Inagaki, Y., Toyoda, K., Shiraishi, T., and Ichinose, Y. (2003a) Post-translational modification of flagellin determines the specificity of HR induction. *Plant Cell Physiol.* **44**: 342-349.

Taguchi, F., Shimizu, R., Nakajima, R., Toyoda, K., Shiraishi, T., and Ichinose, Y. (2003b) Differential effects of flagellins from *Pseudomonas syringae* pv. *tabaci, tomato* and *glycinea* on plant defense response. *Plant Physiol. Biochem.* **41**: 165-174.

Takeuchi, K., Taguchi, F., Inagaki, T., Toyoda, K., Shiraishi, T., and Ichinose, Y. (2003) Flagellin glycosylation island in *Pseudomonas syringae* pv. *glycinea* and its role in host specificity. *J. Bacteriol.* **185**: 6658-6665.

Thibault, P., Logan, S.M., Kelly, J.F., Brisson, J.-R., Ewing, C.P., Trust, T.J., and Guerry. P. (2001) Identification of the carbohydrate moieties and glycosylation motifs in *Campylobacter jejuni* flagellin. *J. Biol. Chem.* **276**: 34862-34870.

Yokoyama, T., Kobayashi, N., Kouchi, H., Minamisawa, K., Kaku, H., and Tsuchiya, K. (2000) A lipochito-oligosaccharide, Nod factor, induces transient calcium influx in soybean suspension-cultured cells. *Plant J.* **22**: 71-78.

Yonekura, K., Maki-Yonekura, S., and Namba, K. (2003) Complete atomic model of the bacterial flagellar filament by electron cryomicroscopy. *Nature* **424**: 643-650.

Figure legends

Fig. 1. Glycosylation island and role of gene products in flagellin glycosylation in *P. syringae* pv. *tabaci* 6605. **A,** Schematic representation of the glycosylation island in a flagella gene cluster. Predicted *orfs* and operons are indicated by boxes and the direction of transcription with arrows. **B,** Northern blot analysis of each *orf* gene in the glycosylation island. **C,** Coomassie brilliant blue staining. **D,** Staining of the glycosyl moiety in purified flagellins. In **B, C** and **D,** lane 1: wild-type, lane 2: Δ*orf1*, lane 3: Δ*orf2*, lane 4: Δ*orf3* mutants. **E,** Complementation of the flagellin glycosylation island assessed by immunoblot analysis. Lane 1: wild-type, lane 2: Δ*orf1*, lane 3: Δ *orf1* possessing pDSKGI, lane 4: Δ*orf1*, possessing pDSK519, lane 5: Δ*orf2*, lane 6: Δ *orf2*, possessing pDSKGI, lane 7: Δ*orf2* possessing pDSK519, lane 8: Δ*orf3*, lane 9: Δ *orf3* possessing pDSKGI, lane 10: Δ*orf3* possessing pDSK519.

Fig. 2. Glycosylated amino acid residues of flagellin protein in *P. syringae* pv. *tabaci* 6605. HPLC profile of flagellin fragments from wild-type (**A**) and Δ*orf1* (**B**) created by aspartic *N*-peptidase digestion. Absorbance at 210 nm is indicated. The peptide fractions numbered 41, 50 and 66, were detected specifically in the digestion of wild-type flagellin. **C**, Determined amino acid sequences of the peptide fractions. A red x indicates an unidentified amino acid. Two

amino acid sequences were determined in one peptide fraction by a difference in molar ratio. **D**, Amino acid sequence of flagellin and of glycosylated residues. The putative N-terminal and C-terminal D0 domains are shown by lower case letters. Putative D1 and D3 domains are shown by upper case letters, and the D3 domain is further indicated by a bidirectional arrow. Sequenced peptides are indicated by the upper lines. Glycosylated amino acids are shown in red letters.

Fig. 3. SDS-PAGE of flagellin proteins from wild-type and the glycosylation mutants. Purified flagellin proteins were stained with coomassie brilliant blue. Lane 1: wild-type, lane 2: Δ*orf1*, lane 3: Δ*orf2*, lane 4: Δ*orf3*, lane 5: S143A mutant, lane 6: S164A mutant, lane 7: S176A mutant, lane 8: S183A mutant, lane 9: S193A mutant, lane 10: S201A mutant, lane 11: six serine-substituted (S143A, S164A, S176A, S183A, S193A and S201A) mutant.

Fig. 4. MALDI-TOF MS analysis of peptide fragments (Asn^{136}-Lys^{255}) of flagellins from *P. syringae* pv. *tabaci* 6605. MALDI *m/z* spectra of peptide Asn^{136}-Lys^{255} of flagellins from the wild-type strain (WT), Δ*orf1*, Δ*orf2*, Δ*orf3* and S143A mutants.

Fig. 5. Comparison of the flagellin structure of *P. syringae* pv. *tabaci* 6605 and *Salmonella*

typhimurium. **A**, Sequence alignment of flagellin from *P. syringae* pv. *tabaci* 6605 (Pst) and from *S. typhimurium* (Sty). Residues that are conserved or conservatively exchanged with respect to the flagellin from *P. syringae* pv. *tabaci* 6605 are marked blue and green, respectively. The horizontal bars under the sequences indicate secondary structure (β-strand in blue and α-helix in red) based on the crystal structure of *Salmonella* flagellin (PDB Id: 1UCU) and a second prediction using Jpred (Cuff *et al.,* 1998) for flagellin from *P. syringae* pv. *tabaci* 6605. Six red asterisks (*) indicate glycosylated amino acid residues. **B**, Comparison of the predicted tertiary structure of flagellin from *P. syringae* pv. *tabaci* 6605 with the crystal structure of *Salmonella* flagellin (PDB Id:1IOI). The glycosylation sites are indicated CPK in magenta**.**

Fig. 6. Swarming motility and adhesion by wild-type and glycosylation mutants from *P. syringae* pv. *tabaci* 6605. **A,** Swarming assay. Bacterial cell densities were adjusted to an OD_{600} of 1.0 with 10 mM $MgSO_4$ and 2 µl aliquots were inoculated on SWM agar plate. Photographs were taken after 24 h at 27°C. **B,** Adhesion assay. An overnight culture of each mutant in LB medium with 10 mM $MgCl_2$ was centrifuged and standardized to 0.1 at OD_{600} in MMMF. Two hundred microliters of each culture and MMMF as control were incubated in microtiter plate wells for 48 h at 27°C. After rinsing of wells, adherent cells were stained with 0.5% crystal

violet. Data shown are the average of five independent experiments. Bacterial strains are indicated as follows: wild-type (WT), orf-deleted mutants (Δ*orf1*, Δ*orf2* and Δ*orf3*), single serine-substituted mutants (S143A, S164A, S176A, S183A, S193A and S201A), the six serine-substituted mutant (6 S/A) and *fliC*-deleted mutant (Δ*fliC*).

Fig. 7. Scanning electron micrograph of the surface of tobacco leaves inoculated with *P. syringae* pv. *tabaci* 6605 wild-type (**A**) and Δ*orf1* mutant (**B**). Leaves were incubated for 8 days at 23°C. The bars represent 5 μm.

Fig. 8. Inoculation test of wild-type and *P. syringae* pv. *tabaci* 6605 glycosylation mutants on host tobacco leaves (**A**). Tobacco leaves were spray-inoculated at 2 x 10^8 cfu/ml and incubated at 23°C for 12 days. Photos show representative results obtained from four independent experiments. Bacterial growth in tobacco leaves inoculated by spray-method at 2 x 10^8 cfu/ml (**B**) or infiltration method at 2 x 10^5 cfu ml^{-1} (**C**) with the wild-type strain (WT), Δ*orf1*, Δ*orf2*, Δ*orf3* and S183A mutants and the six serine-substituted mutant (6 S/A). Bacterial populations were calculated at 1, 3 and 8 days post-inoculation. The bars represent standard deviations for four independent experiments.

Fig. 9. Defense response of soybean cells to flagellins from mutant strains of *P. syringae* pv. *tabaci* 6605. The ratio of dead cells in suspension-cultured soybean cells was measured after treatment with flagellin at a final concentration of 0.32 μM or the corresponding preparation from the Δ*fliC* mutant of *P. syringae* pv. *tabaci* 6605. The bars represent standard deviations for four independent experiments. Bacterial strains *P. syringae* pv. *tabaci* and pv. *glyciena* each wild-type are indicated as Pst WT and Psg WT, respectively. Other strains are indicated in the legend of Fig. 6.

Table 1. Molecular masses of intact flagellin and peptide fragment (N^{136}-K^{255})

P. syringae	Intact (A^{2}-Q^{282})[*1]			fragment (N^{136}-K^{255})		
	Measured $[M+H]^+$ (Da) [*2]	Predicted $[M+H]^+$ (Da) [*3]	Δ [(*2-*3)]	Measured $[M+H]^+$ (Da) [*2]	Predicted $[M+H]^+$ (Da) [*3]	Δ [(*2-*3)]
pv. *tabaci* WT	32382, 32529	29148	3234, 3381	15301, 15447	12074	3227, 3373
S143A	31850, 31997	29132	2718, 2865	14743, 14890	12058	2685, 2832
S164A	31827, 31967	29132	2695, 2835	14746, 14892	12058	2688, 2834
S176A	31856, 32006	29132	2724, 2874	14749, 14893	12058	2691, 2835
S183A	31860	29132	2728	14748, 14895	12058	2690, 2837
S193A	31817, 31973	29132	2685, 2841	14750, 14898	12058	2692, 2840
S201A	31837, 31983	29132	2705, 2851	14745, 14890	12058	2687, 2832
6 S/A	- [*4]	29052	- [*4]	11980	11978	2
Δorf1	29145	29148	-3	12073	12074	-1
Δorf2 [*5]	29273-31427	29148	125-2279	12220-14367	12074	146-2293
Δorf3	32370, 32518	29148	3222, 3370	15298, 15445	12074	3224, 3371

[*1]: Because the N-terminal sequence of purified flagellin elicitor began at A2 (Taguchi *et al*., 2003b), there is no translation start codon (Met) in the mature filament. [*2]: Major molecular masses measured by MALDI-TOF mass spectrometer. [*3]: Molecular mass predicted by deduced amino acid sequence. [*4]: not determined. [*5]: Measured molecular masses were not heterogeneous.

Table 2. Bacterial strains used in this study

Bacterial strain	Relevant characteristics[a]	Reference or source
E. coli		
DH5a	*F⁻λ⁻ø80dlacZΔM15 Δ(lacZYA-argF)U169 recA1 endA1 hsdR17(rK⁻ mK⁺) supE44 thi-1 gyrA relA1*	Takara, Kyoto, Japan
S17-1	*thi pro hsdR⁻hsdM⁺recA [chr::RP4-2-Tc::Mu-Km::Tn7]*	Schäfer *et al.* 1994
P. syringae pv. *tabaci*		
Isolate 6605	Wild-type, Nal^r	Shimizu *et al.* 2003
6605-dC	Isolate 6605 Δ*fliC*	Shimizu *et al.* 2003
6605-d1	Isolate 6605 Δ*orf1*	This study
6605-d2	Isolate6605 Δ*orf2*	This study
6605-d3	Isolate 6605 Δ*orf3*	This study
6605-S143A	Isolate 6605 S143A	This study
6605-S164A	Isolate 6605 S164A	This study
6605-S176A	Isolate 6605 S176A	This study
6605-S183A	Isolate 6605 S183A	This study
6605-S193A	Isolate 6605 S193A	This study
6605-S201A	Isolate 6605 S201A	This study
6605-6 S/A	Isolate 6605 S143A, S164A, S176A, S183A, S193A, S201A	This study
Plasmids		
pMC	1.8-kb chemeric PCR product deleting *fliC* cloned into pK18*mobSacB* at EcoRI site, Km^r	Shimizu *et al.* 2003
pK18*mobsacB*	Small mobilizable vector, Km^r, sucrose sensitive (*sacB*)	Schäfer *et al.* 1994
pM1a	2.18-kb chimeric PCR product deleting *orf1* cloned into pK18*mobsacB* at EcoRI site	This study
pM2	1.79-kb chimeric PCR product deleting *orf2* cloned into pK18*mobsacB* at EcoRI site	Takeuchi *et al.* 2003
pM3	1.69-kb chimeric PCR product deleting *orf3* cloned into pK18mobsacB at EcoRI site	Takeuchi *et al.* 2003
pDSK519	Broad-host-range cloning vector, Km^r	Keen *et al.* 1988
pDSKG1	9-kb HindIII fragment contaning *orf1, orf2* and *orf3* genes from *P. syringae* pv. *tabaci* 6605 in pDSK519, Km^r	This study

[a] Amp^r = ampicillin resistance; Km^r = kanamycin resistance, Nal^r = nalidixic acid resistance

Fig. 1
Taguchi et al.

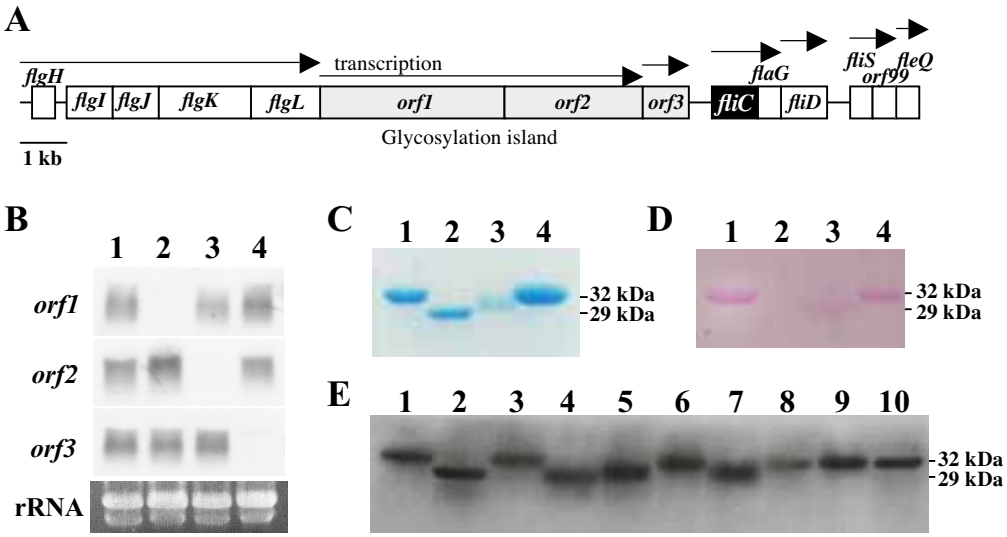

Fig. 2
Taguchi et al.

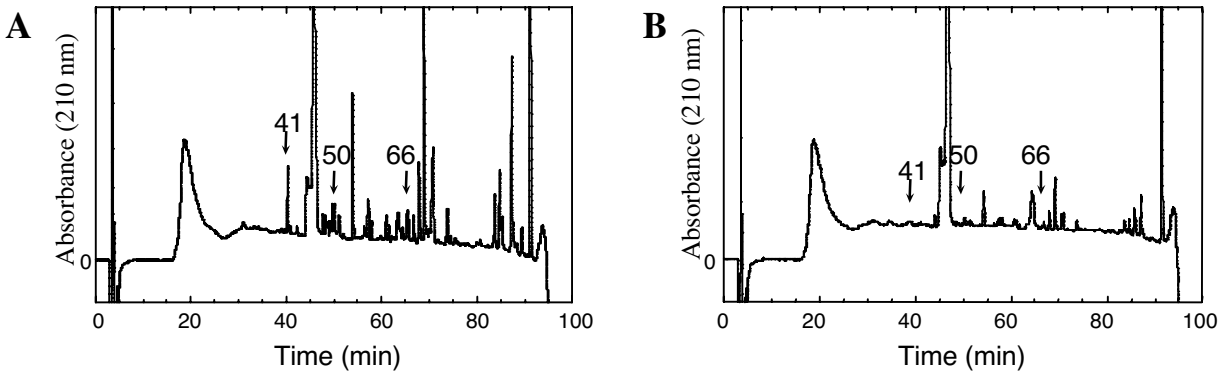

C

Fr.41-1 ^{200}DxALQTINSTRA
Fr.41-2 ^{70}DGMSLAQTA
Fr.50-1 ^{23}DALSTSMTRLSSGLKINSAK
Fr.50-2 ^{168}DANTLGVGxAVTIAGxDSTT
Fr.66-1 ^{189}ETNFxAAIAAI
Fr.66-2 ^{139}DGSAxTMTFQVGSNSGASNQITLTL

D

Fr.50-1
maltvntnva slnvqknlgr asdalstsmt rlssglkins akddaaglqi atkits**QIRG** 60

Fr.41-2
QTMAIKNAND GMSLAQTAEG ALQESTNILQ RMRELAVQSR NDSNSSTDRD ALNKEFTAMS 120

Fr.66-2 Fr.50-2
SELTRIAQST NLNGKNLLDG SASTMTFQVG SNSGASNQIT LTLSASFDAN TLGVGSAVTI 180

Fr.66-1 Fr.41-1
AGSDSTTAET NFSAAIAAID SALQTINSTR ADLGAAQNRL TSTISNLQNI NENASAALgr 240

vqdtdfaaet aqltkqqtlq qastsvlaqa nqlpsavlkl lq 282

Fig. 3
Taguchi et al.

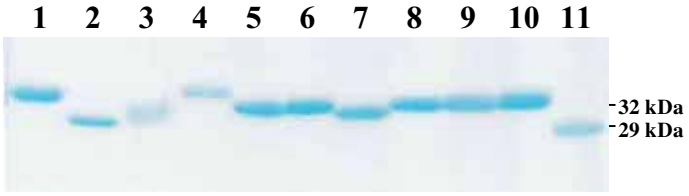

Fig. 4
Taguchi et al.

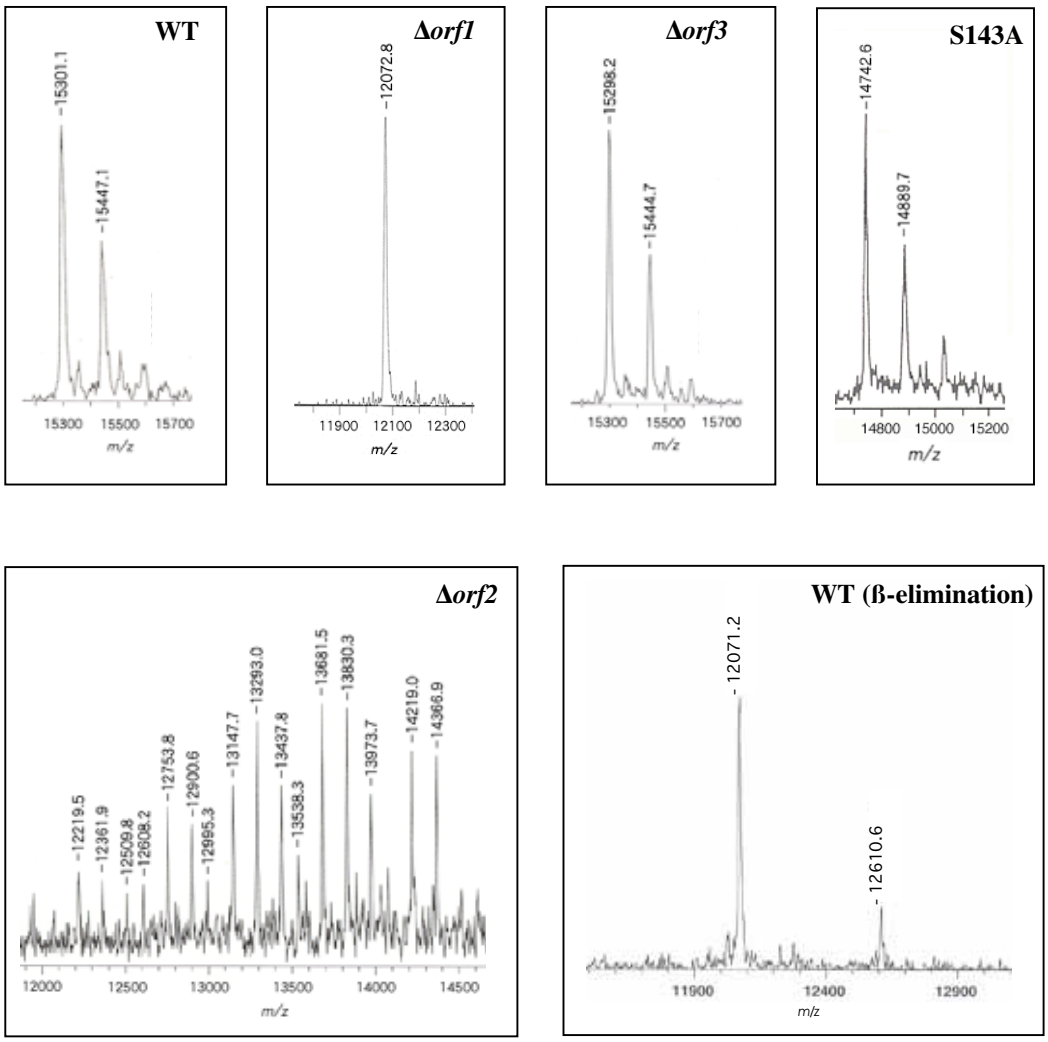

Fig. 5
Taguchi et al.

A

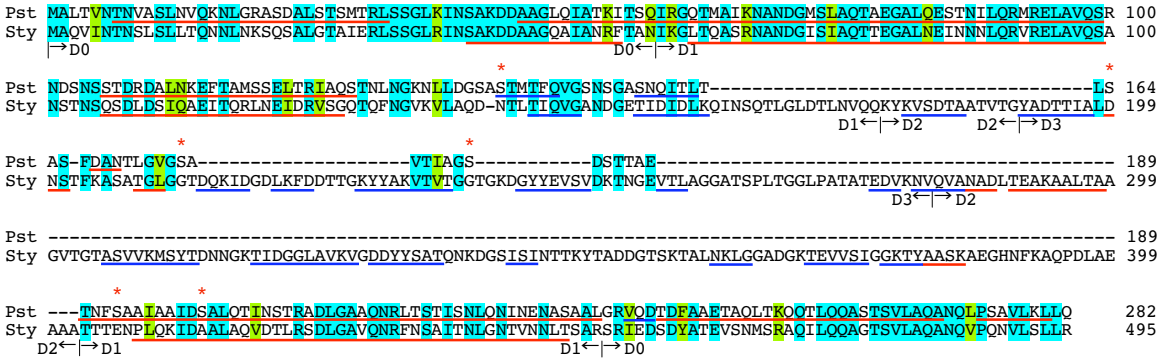

B

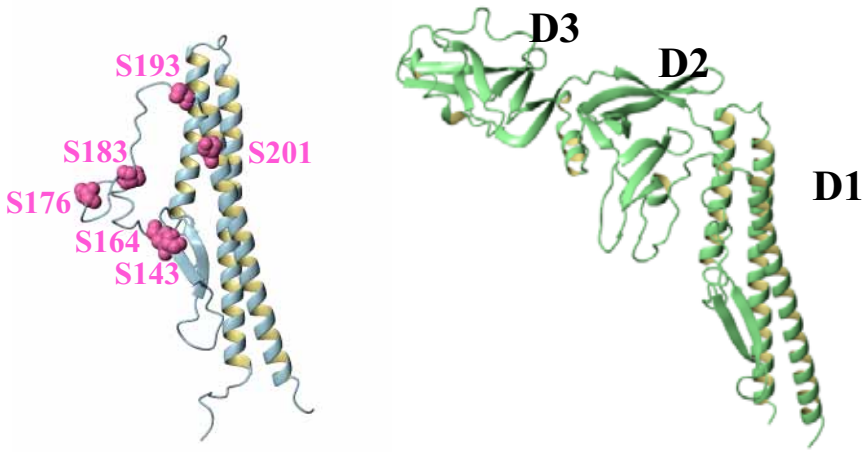

P. s.* pv. *tabaci ***S. typhimurium***

Fig. 6
Taguchi et al.

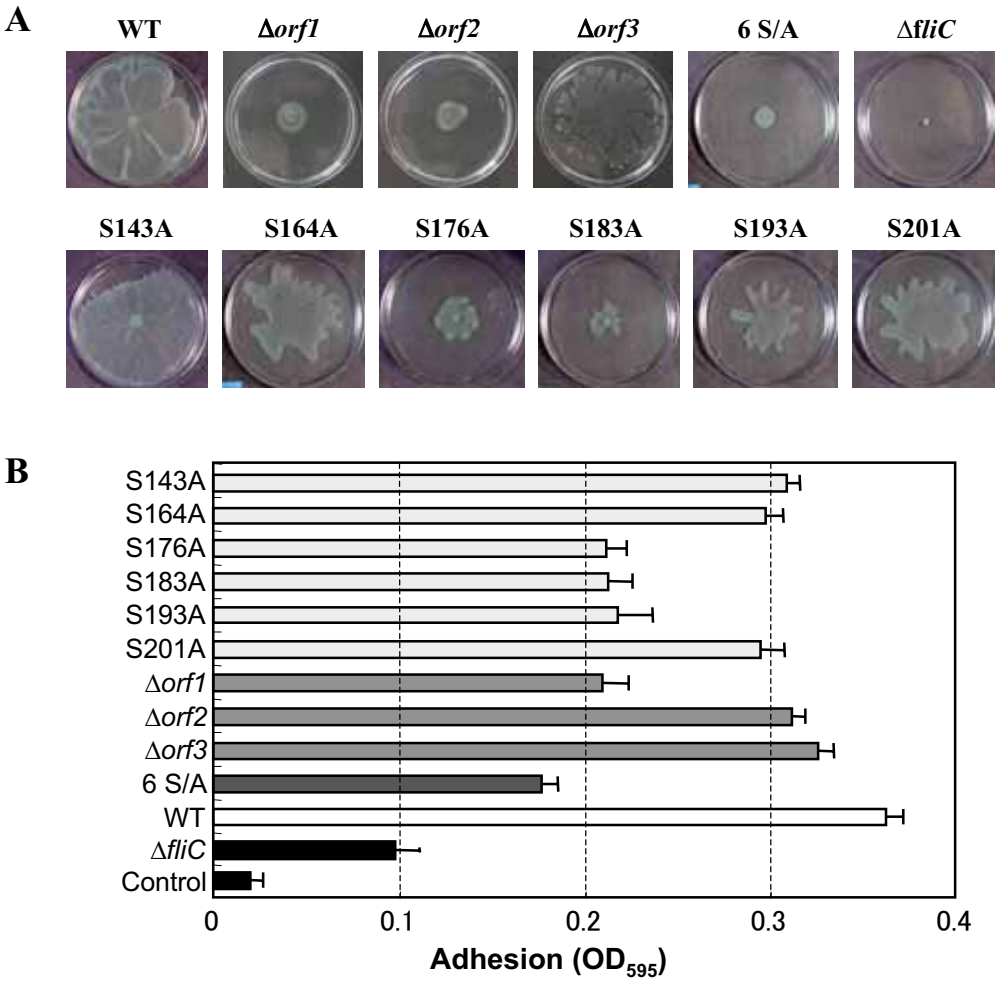

Fig. 7
Taguchi et al.

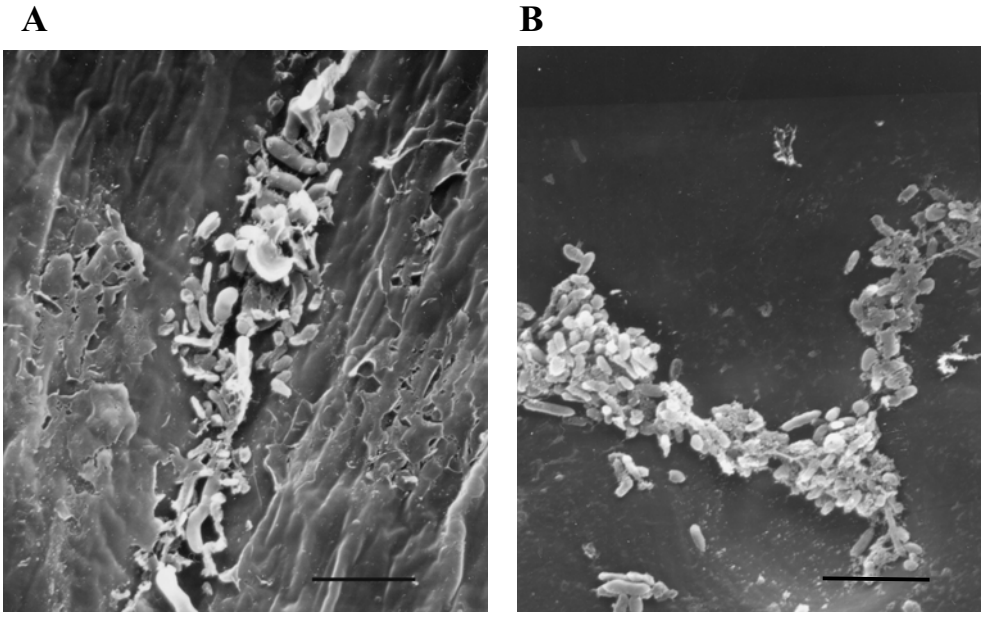

Fig. 8
Taguchi et al.

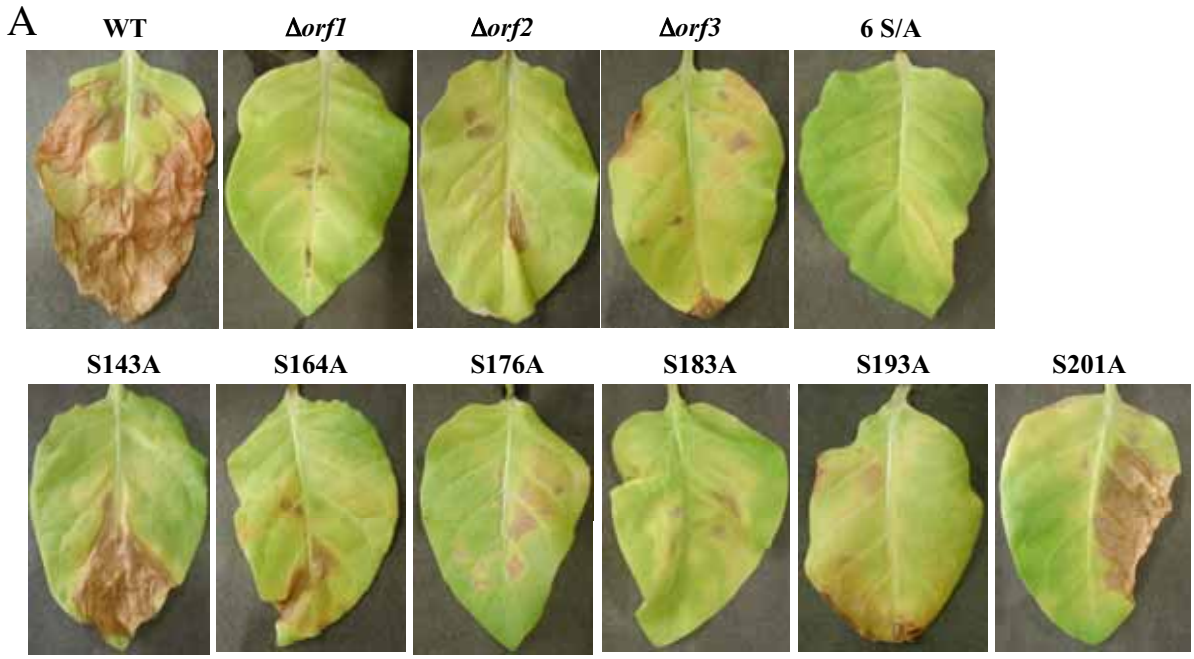

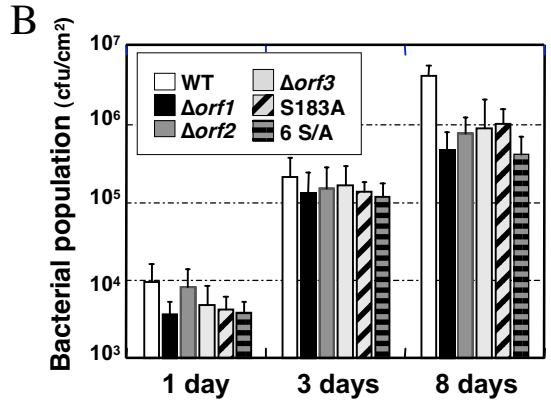

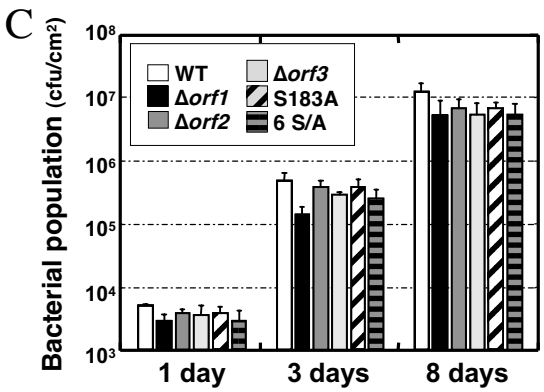

Fig. 9
Taguchi et al.